Received: 6 May 2018 | Revised: 26 June 2018 | Accepted: 27 June 2018

DOI: 10.1002/mrm.27457

FULL PAPER

Magnetic Resonance in Medicine

Gradient-echo and spin-echo blood oxygenation level–dependent functional MRI at ultrahigh fields of 9.4 and 15.2 Tesla

SoHyun Han[1,*] | Jeong Pyo Son[1,2,*] | HyungJoon Cho[3] | Jang-Yeon Park[1,4] | Seong-Gi Kim[1,2,4]

[1]Center for Neuroscience Imaging Research, Institute for Basic Science (IBS), Suwon, South Korea

[2]Department of Health Sciences and Technology, Samsung Advanced Institute for Health Sciences and Technology, Sungkyunkwan University, Seoul, South Korea

[3]Department of Biomedical Engineering, Ulsan National Institute of Science and Technology, Ulsan, South Korea

[4]Department of Biomedical Engineering, Sungkyunkwan University, Suwon, South Korea

Correspondence
Seong-Gi Kim, Center for Neuroscience Imaging Research, N Center, Sungkyunkwan University, Suwon 16419, South Korea
Email: seonggikim@skku.edu

Current address
SoHyun Han, Athinoula A. Martinos Center for Biomedical Imaging, MGH/Harvard Medical School, Charlestown, Massachusetts.

Funding information
Institute for Basic Science, Grant/Award Number: IBS-R015-D1

Purpose: Sensitivity and specificity of blood oxygenation level–dependent (BOLD) functional MRI (fMRI) is sensitive to magnetic field strength and acquisition methods. We have investigated gradient-echo (GE)- and spin-echo (SE)-BOLD fMRI at ultrahigh fields of 9.4 and 15.2 Tesla (T).

Methods: BOLD fMRI experiments responding to forepaw stimulation were performed with 3 echo times (TE) at each echo type and B_0 in α-chloralose–anesthetized rats. The contralateral forelimb somatosensory region was selected for quantitative analyses.

Results: At 9.4 T and 15.2 T, average baseline T_2^* (n = 9) was 26.6 and 17.1 msec, whereas baseline T_2 value (n = 9) was 35.7 and 24.5 msec, respectively. Averaged stimulation-induced ΔR_2^* was –1.72 s^{-1} at 9.4 T and –3.09 s^{-1} at 15.2 T, whereas ΔR_2 was –1.19 s^{-1} at 9.4 T and –1.97 s^{-1} at 15.2 T. At the optimal TE of tissue T_2^* or T_2, BOLD percent changes were slightly higher at 15.2 T than at 9.4 T (GE: 7.4% versus 6.4% and SE: 5.7% versus 5.4%). The ΔR_2^* and ΔR_2 ratio of 15.2 T to 9.4 T was 1.8 and 1.66, respectively. The ratio of the macrovessel-containing superficial to microvessel-dominant parenchymal BOLD signal was 1.73 to 1.76 for GE-BOLD versus 1.13 to 1.19 for SE-BOLD, indicating that the SE-BOLD contrast is less sensitive to macrovessels than GE-BOLD.

Conclusion: SE-BOLD fMRI improves spatial specificity to microvessels compared to GE-BOLD at both fields. BOLD sensitivity is similar at the both fields and can be improved at ultrahigh fields for thermal-noise–dominant ultrahigh-resolution fMRI.

KEYWORDS
BOLD, fMRI, gradient-echo, spin-echo, ultrahigh field

*SoHyun Han and Jeong Pyo Son contributed equally to this work.

1 | INTRODUCTION

Blood oxygenation level–dependent (BOLD) contrast[1] is mainly used in functional MRI (fMRI) investigations.[2–4] It is well known that the BOLD effect is sensitive to vascular parameters, such as venous blood volume, vessel size, and vessel orientation,[5–7] whose contributions may vary with the magnetic field strength or acquisition methods.[8] Field dependence studies have been reported that higher BOLD signal was observed at 4 Tesla (T) than at 1.5 T[9–11] and at 7 T than at 4 T.[12] This observation has inspired researchers to pursue ultrahigh field MRI for achieving the better sensitivity of the BOLD signal.

At ultrahigh magnetic fields of > 7 T, only 1 experimental result was reported for comparing field-dependent BOLD responses. When the same echo time (TE) was used for 7 T and 11.7 T, the BOLD percent change was similar,[13] suggesting that stimulation-induced relaxation rate changes (− % change/TE; ΔR_2^* and ΔR_2) are independent of magnetic field strength (B_0). Extensive Monte Carlo simulation of ultrahigh field BOLD contrasts showed that ΔR_2^* and ΔR_2 (ie, percent changes at the same TE) increase with B_0, but at optimal TE, which is dependent on B_0, the BOLD signal is similar at $B_0 > 7$ T.[14] These expectations[14] are inconsistent with experimental data.[13] Thus, it is important to further examine field-dependent BOLD contrasts at ultrahigh fields.

Specificity of BOLD fMRI to microvessels increases with B_0. According to the BOLD model,[5,6,14–17] the extravascular (EV) BOLD contribution from macrovasculature is linearly dependent on B_0, whereas the EV contribution from microvasculature increases supralinearly with B_0. Thus, higher magnetic fields increase the relative contribution of the microvascular EV component to the BOLD signals. The contribution of macrovascular component to BOLD fMRI can be reduced in spin-echo (SE) sequences because the EV components of large vessels are mostly refocused by 180° radiofrequency (RF) pulse. Thus, SE-BOLD fMRI has been suggested for high-resolution fMRI at ultrahigh fields.[12,18]

The purpose of this work was to experimentally investigate the BOLD signal at ultrahigh magnetic field strengths (9.4 T and 15.2 T) and echo types (gradient-echo (GE) and SE). Multiple TE GE- and SE-BOLD fMRI studies were performed in a well-known forepaw stimulation rat model[19–22] for determining field-dependent GE- and SE-BOLD contrasts experimentally. Stimulation-induced $\Delta R_2^*/\Delta R_2$ was measured for examining biophysics of BOLD fMRI.[23–28]

2 | METHODS

2.1 | Animal preparation and forepaw stimulation

A total of 18 male Sprague–Dawley rats, weighing between 243 and 432 g, were used with approval from the Institutional Animal Care and Use Committee of Sungkyunkwan University (Suwon, South Korea). Rats were initially anesthetized with 4% isoflurane (Ifran; Hana Pharm. Co., Ltd., Seoul, Korea) in 100% oxygen, and intubation was performed for mechanical ventilation (TOPO; Kent Scientific, Torrington, CT). The anesthesia level was reduced to 2% during surgical preparation, and 100% O_2 inhalation gas was changed to oxygen-enriched air (~30% O_2). Catheters were inserted into the femoral artery and vein for monitoring arterial blood pressure, withdrawing arterial blood, and delivering α-chloralose (80 mg/kg was administered by bolus injection followed by 40 mg/kg/90 min), respectively. The head of the rat was fixed in a home-built cradle with 2 ear bars, a bite bar, and a mask to reduce the head motion shown in Supporting Information Figure S1. Ear bars were designed to connect with detachable extension bars. After positioning the animal in the cradle, the extension bars were removed for minimizing the head-holder size. Body temperature was kept constant at 37 ± 1°C by using a rectal temperature probe and a temperature-controlled water blanket. Arterial blood gases (pO_2, pCO_2, and pH) were measured by a portable blood gas analyzer (i-STAT Portable Clinical Analyzer; Abbott Point of Care Inc, Princeton, NJ). Ventilation rate and volume were adjusted to maintain an arterial carbon dioxide partial pressure level between 30 and 40 mm Hg.

For electrical stimulation, 2 pairs of needle electrodes were inserted between digits 1 and 3 under the skin of the right and left forepaws and connected to a current stimulator (Isoflex; AMPI, Jerusalem, Israel). Somatosensory stimulation was delivered using a constant current isolator (Iso-Flex; AMPI) to 1 forepaw, and its stimulation parameters were 1.5 mA (current), 300 μsec (pulse duration), and 3 Hz (repetition rate), which has been commonly used for forepaw stimulation in α-chloralose–anesthetized rats.[22]

2.2 | Functional magnetic resonance imaging

MR experiments were performed on 2 high-field Bruker MR instruments (Paravision 6; Bruker Biospec, Billerica, MA); a 9.4-T/30-cm MRI with an actively shielded 12-cm inner diameter (ID) gradient insert operating at a maximum gradient strength of 66 Gauss/cm with a rise time of 141 μsec, and a 15.2-T/11-cm MRI with an actively shielded 6-cm ID gradient operating at a maximum gradient strength of 100 Gauss/cm with a rise time of 110 μsec. A combination of 86-mm ID birdcage for RF transmission and 20-mm ID surface coil for RF reception was used at 9.4 T, whereas a 20-mm ID surface coil was for RF excitation and reception at 15.2 T. After positioning the slice of interest containing the primary somatosensory cortex at the center of the magnetic field, a magnetic field homogeneity was optimized by both global shimming and volume-localized shimming routines. Initially, scout GE-BOLD fMRI studies of 20-second forepaw stimulation were performed for choosing the right or left

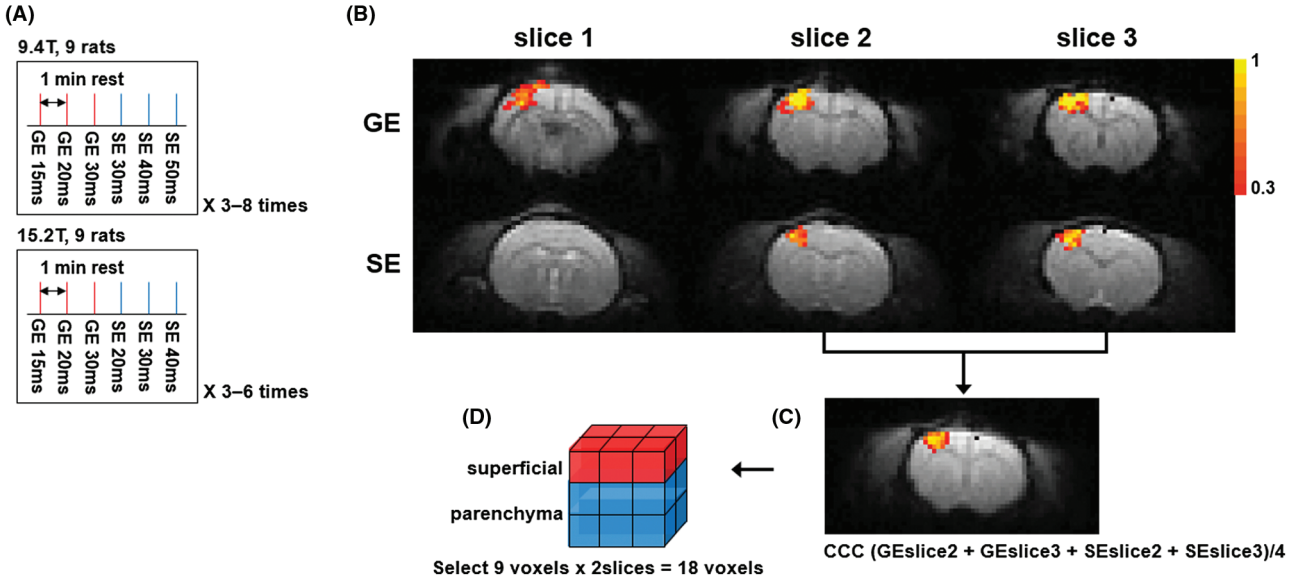

FIGURE 1 (A) Experimental protocol of 9.4 T and 15.2 T. Three TE GE-BOLD runs and 3 TE SE-BOLD runs were performed sequentially. The protocol was repeated 3 to 8 times. Each BOLD run was separated by a rest of 1 minute. (B) Statistical maps with GE- (TE = 20 msec) and SE-BOLD (TE = 40 msec) overlaid on corresponding BOLD images at 9.4 T. Color bar represents the cross-correlation values. (C) Averaged CCC map from 2 selected slices of GE- and SE-BOLD overlaid on averaged BOLD images. (D) Selected 9 voxels by 2 slices. The superficial ROI was selected as a region with 3 superficial voxels by 2 slices (red), and the parenchyma ROI was selected as a region with 6 inner voxels by 2 slices (blue)

primary somatosensory cortex (eg, left or right forepaw stimulation) and slice positions. Then, three 1-mm-thick slices with the highest responses were chosen for systematic studies. All fMRI data were obtained using a single-shot GE or SE echo-planar imaging (EPI) sequence with a matrix size of 64×32, field of view of 3.0×1.5 cm^2, 3 consecutive slices of 1-mm thickness, bandwidth of 170.5 kHz, and repetition time of 2 seconds. Because a surface coil was used for 15.2 T SE-BOLD studies, the 180° RF pulse power was optimized for maximizing MR intensity at the primary somatosensory cortex.

Nine animals were used for each magnetic field, and 3 TEs were used to determine ΔR_2^* and ΔR_2 for fMRI studies. Three TEs were 15, 20, and 30 msec for GE-BOLD at both fields, whereas SE-BOLD TEs were 30, 40, and 50 msec for 9.4 T, and 20, 30, and 40 msec for 15.2 T. Each fMRI run consisted of a 40-seconds resting period, followed by 20 seconds of forepaw stimulation and 40 seconds of rest. Each fMRI session block consisted of 3 GE-BOLD runs and 3 SE-BOLD runs with different TE values sequentially as shown in Figure 1A and was repeated 3 to 8 times. Each fMRI run was separated by a rest of 1 minute as shown in Figure 1A.

2.3 | fMRI data analysis

All the data were analyzed using the AFNI software package (https://afni.nimh.nih.gov/afni/) and Matlab (The Mathworks, Inc, Natick, MA). Rigid-body motion correction was performed for all GE- and SE-BOLD fMRI runs using the AFNI software package. The reference for motion correction was set as the baseline GE-EPI image at TE of 15 msec of the first session. As a result, GE- and SE-BOLD fMRI runs with multiple TEs were aligned to the reference image. Multiple fMRI runs with identical experimental parameters were averaged. Then, cross-correlation coefficients (CCCs) were obtained on a voxel-by-voxel basis using a boxcar cross-correlation method,[29] and thresholded with the CCC threshold of 0.3 and the minimum cluster size of 3 voxels (effective P value was < 0.05). All quantitative values are reported as mean ± standard errors of mean.

2.3.1 | Section of the region of analysis

To determine a common region of interest (ROI) in each animal, both GE- (TE = 20 msec at 9.4 T and 15 msec at 15.2 T) and SE-BOLD (TE = 40 msec at 9.4 T and 30 msec at 15.2 T) statistical maps were combined as shown in Figure 1C. Optimal TEs were selected for each echo type based on literature (Equations 5 and 6 of Uludağ et al[14]). Two slices with higher CCC values were chosen out of 3 slices for selecting consistent slice positions across animals. CCC maps of 2 slices were averaged as shown in Figure 1C. Note that the highest CCC values in the merged maps were near the center of activation area.

Three ROIs were chosen. (1) Nine voxels were chosen from the center of the highest CCC value and consequently 18 voxels (9 voxels × 2 slices) were selected. This ROI corresponded approximately to the primary somatosensory forelimb cortex (S1FL) based on the stereotaxic coordinate.[30] This S1FL ROI was divided into 2 ROIs, superficial and parenchyma. (2) The superficial ROI was a region with 3 superficial voxels × 2 slices, which contained parenchymal and pial vessels (red voxels in Figure 1D). (3) The parenchyma ROI was a region with 6 inner voxels × 2 slices, which contained mostly parenchymal microvasculature (blue voxels in Figure 1D).

2.3.2 | Quantitative analyses

All quantitative analyses were performed at a ROI basis. BOLD time courses were obtained from ROIs in each animal. (1) Baseline T_2^* and T_2 of brain tissue were calculated by fitting logarithmic TE-dependent GE- and SE-BOLD signal intensities obtained during the prestimulus baseline from the S1FL ROI to a linear function. (2) BOLD percent signal change was calculated as (mean signal of activation duration – mean signal of prestimulus baseline)/(mean signal of prestimulus baseline) × 100 (%), where the activation duration was defined as the period of 6 to 20 seconds after onset of stimulation. In addition, poststimulus BOLD undershoot percent signal change was calculated by setting the undershoot duration as the period of 10 to 30 seconds after the offset of stimulation. (3) To calculate stimulation-induced ΔR_2^* or ΔR_2, TE-dependent BOLD percent signal changes were plotted as a function of TE and fitted by a linear function. A slope of the linearly fitted line is $-\Delta R_2^*$ or $-\Delta R_2$, whereas an intercept is related to non-TE-dependent responses including inflow effects.

3 | RESULTS

3.1 | Baseline relaxation time and TE dependence of BOLD contrast

All animals were maintained at a normal physiological condition. Mean carbon dioxide partial pressure level was 35.0 ± 3.6 mm Hg ($n = 18$), and oxygen partial pressure level was 155.4 ± 10.0 mm Hg ($n = 18$). Baseline T_2^* and T_2 values were obtained from the S1FL ROI. Baseline T_2^* values were 26.6 ± 3.3 msec ($n = 9$) at 9.4 T and 17.1 ± 2.3 msec ($n = 9$) at 15.2 T, whereas baseline T_2 values were 35.7 ± 0.8 msec ($n = 9$) at 9.4 T and 24.5 ± 0.4 msec ($n = 9$) at 15.2 T. Our experimental values agree with the expected values obtained from Uludağ et al[14] ($T_2^* = 29.2$ and 15.0 msec, and $T_2 = 41.5$ and 22.3 msec for 9.4 T and 15.2 T, respectively). Our 9.4 T T_2 value is similar to the value obtained with the double-spin-echo EPI sequence and 12 different TEs under the same experimental condition, 38.6 ± 2.1 msec ($n = 16$).[18]

TE-dependent GE- and SE-BOLD fMRI studies were performed on both 9.4 T and 15.2 T. One representative animal's data for each magnetic field are shown in Figure 2 for BOLD percent change maps (see Supporting Information Figure S2 for cross-correlation maps). Percent activation maps were overlaid on original EPI images. In both ultra-high magnetic fields, high-quality EPI images were acquired and activation voxels were observed only at the contralateral primary somatosensory cortex. To compare contrast-to-noise ratio (CNR) between TEs and echo type, mean t-value of the S1FL ROI was calculated in each animal and is reported in Table 1. SE-BOLD fMRI had statistically lower t-value than GE-BOLD fMRI ($P < 0.05$), and no statistical difference of BOLD signals between different TEs and between the 2 magnetic fields was observed.

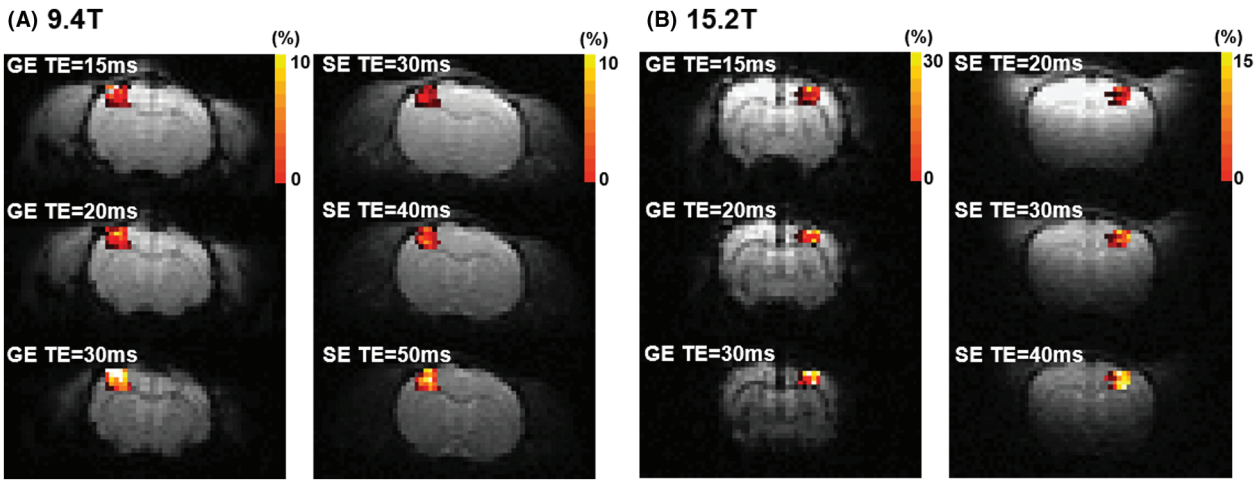

FIGURE 2 Statistical activation maps from 3 TE GE- and SE-BOLD overlaid on the corresponding EPI images at 9.4 T (A) and 15.2 T (B). Color bar represents percent changes

TABLE 1 Averaged t-value of the primary somatosensory forelimb cortex region

	GE-BOLD			SE-BOLD		
9.4 T ($n = 9$)	15 msec	20 msec	30 msec	30 msec	40 msec	50 msec
	5.84 ± 0.23	6.21 ± 0.15	6.20 ± 0.15	4.47 ± 0.24	4.84 ± 0.22	4.96 ± 0.23
15.2 T ($n = 9$)	15 msec	20 msec	30 msec	20 msec	30 msec	40 msec
	5.64 ± 0.25	5.89 ± 0.36	5.64 ± 0.33	4.37 ± 0.37	4.47 ± 0.37	4.67 ± 0.30

No statistical difference was found ($P > 0.5$) between echo times in the same field and sequence using repeated 1-way analysis of variance test.

3.2 | Magnetic field strength and echo-type dependencies of BOLD fMRI signal change

TE-dependent percent signal changes can be used to separate TE-dependent and -independent components. BOLD fMRI time courses were obtained from the S1FL ROI and are shown in Figure 3A to 3D. BOLD signals increased rapidly after stimulation onset and peaked at ~6 seconds. After the stimulus offset, a small poststimulus undershoot was observed for GE- and SE-BOLD fMRI time courses (see red horizontal bar area in time courses). Positive BOLD response increases with TE and magnetic field strength. However, the poststimulus undershoot is not significantly related to magnetic field strength and echo type, whereas a slightly larger poststimulus undershoot was observed at a longer TE (see Supporting Information Table S1). To compare GE- (red) and SE-BOLD (blue) signal changes at 9.4 T (filled circle) and 15.2 T (open circle), BOLD percent signal changes as a function of TE were tabulated in Table 2 and plotted in Figure 3E. When TE = T_2^* or T_2 from our observation, BOLD percent change was calculated by a linear interpolation of percent changes at an appropriate TE. BOLD percent changes were slightly higher at 15.2 T than at 9.4 T; GE-BOLD signal change was 6.4% at 9.4 T versus 7.4% at 15.2 T, whereas the SE-BOLD signal change was 5.4% at 9.4 T versus 5.7% at 15.2 T. Within TEs chosen in our studies, BOLD percent signal changes showed a linear dependency on TE with a close-to-zero intercept, indicating that the nonlinear TE component is minimal. Intercept values were observed lower in SE-BOLD for both magnetic fields compared to those in GE-BOLD, which indicate smaller inflow effects in SE-BOLD fMRI.

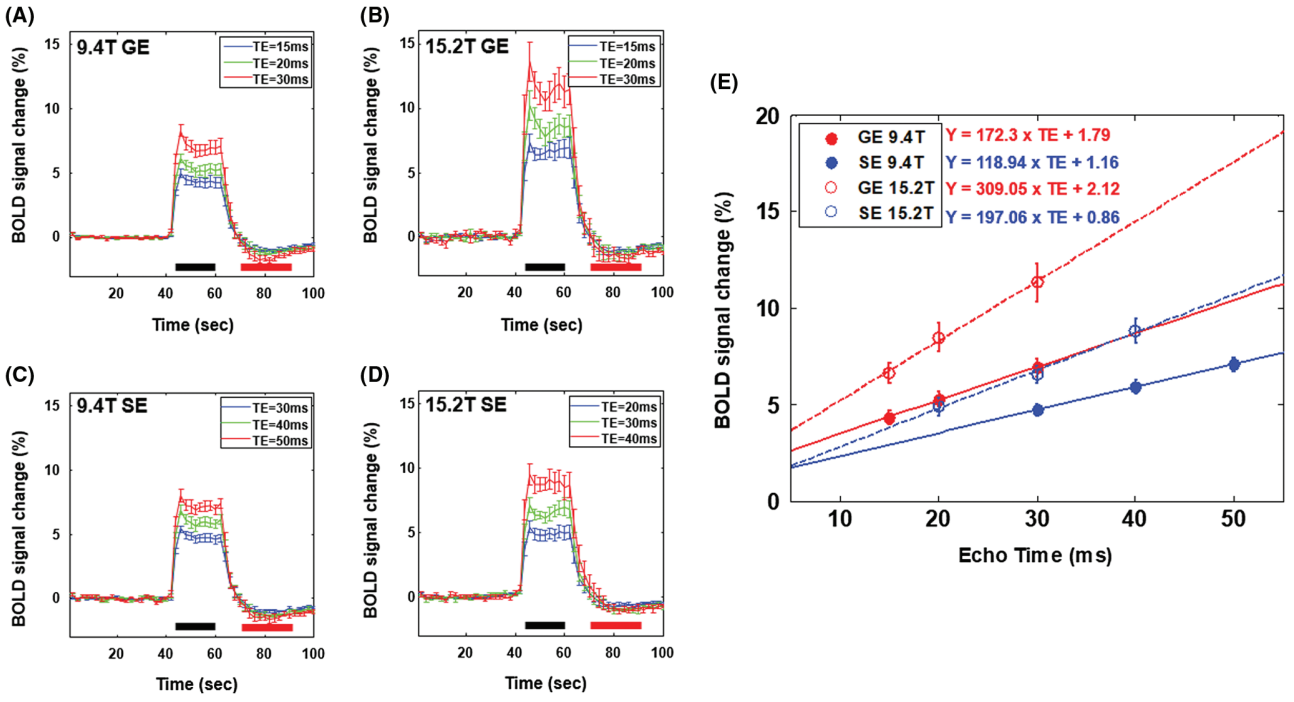

FIGURE 3 (A), (B) GE-BOLD fMRI time courses obtained from the S1FL ROI ($n = 9$) for TE of 15 msec (blue), 20 msec (green), and 30 msec (red) at 9.4 T and 15.2 T, respectively. (C) SE-BOLD fMRI time courses obtained from the S1FL ROI ($n = 9$) for TE of 30 msec (blue), 40 msec (green), and 50 msec (red) at 9.4 T. (D) SE-BOLD fMRI time courses obtained from the S1FL ROI ($n = 9$) for TE of 20 msec (blue), 30 msec (green), and 40 msec (red) at 15.2 T. Activation duration was defined as the period of 6 to 20 seconds after the onset of stimulation at time = 40 seconds (black horizontal bar), and poststimulus duration was defined as the period of 10 to 30 seconds after the offset of stimulation at time = 60 seconds (red horizontal bar). (E) TE-dependent BOLD percent signal changes for GE (red) and SE (blue) at 9.4 T (filled circle) and 15.2 T (open circle). Fitted lines by a linear function were overlapped with solid lines (9.4 T) and dashed lines (15.2 T)

TABLE 2 GE- and SE-BOLD percent signal changes at multiple TEs at 9.4 T and 15.2 T

%	GE-BOLD				SE-BOLD			
9.4 T ($n = 9$)	15 msec	20 msec	30 msec	ΔR_2^* (s^{-1})	30 msec	40 msec	50 msec	ΔR_2 (s^{-1})
	4.33 ± 0.35	5.3 ± 0.39	6.94 ± 0.46	−1.72 ± 0.13	4.72 ± 0.29	5.92 ± 0.35	7.11 ± 0.37	−1.19 ± 0.09
15.2 T ($n = 9$)	15 msec	20 msec	30 msec	ΔR_2^* (s^{-1})	20 msec	30 msec	40 msec	ΔR_2 (s^{-1})
	6.64 ± 0.54	8.48 ± 0.73	11.33 ± 0.98	−3.09 ± 0.35*	4.9 ± 0.43	6.56 ± 0.45	8.84 ± 0.63	−1.97 ± 0.15*

Nonpaired t-test was performed between ΔR_2^* (ΔR_2) values of 2 magnetic fields (*$P < 0.001$).

3.3 | BOLD signal change in superficial and parenchyma regions

BOLD percent signal change is sensitive to baseline blood volume and vessel size. In GE-BOLD signals, areas with the high BOLD percent signal changes are located along the surface of the cortex (see Figure 2). However, in SE-BOLD signals, those are located in both the surface and deep cortex. To examine the sensitivity and specificity of BOLD fMRI quantitatively, the S1FL ROI was divided into the superficial ROI containing macrovasculature and the parenchyma ROI with microvasculature. BOLD percent signal changes obtained from 2 ROIs are plotted as a function of TE in Figure 4. As expected, the superficial ROI (red) had higher percent changes as well as steeper slope than the parenchyma ROI (blue), especially for GE-BOLD fMRI (solid line) in both fields. Stimulation-induced ΔR_2^* and ΔR_2 were obtained from the fitted slopes and are tabulated in Table 3. Ratios of relaxation rates in the superficial ROI to the parenchyma ROI (super/par ratio) were reported as well as ratios at 15.2 T to 9.4 T (15.2 T/9.4 T). Both ΔR_2^* and ΔR_2 are higher in the superficial ROI compared to the parenchyma ROI ($P < 0.05$), indicating that the superficial ROI has higher baseline total and microvascular cerebral blood volume CBV. As expected, $\Delta R_2^*/\Delta R_2$ of the parenchyma ROI is less than that of the superficial ROI.

4 | DISCUSSION

Our major findings are (1) BOLD ΔR_2 increases linearly with magnetic field strength, and ΔR_2^* increases supralinearly

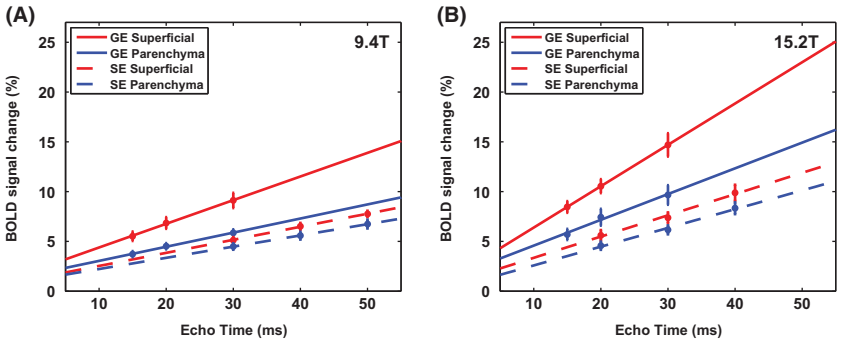

FIGURE 4 TE-dependent GE- (solid line) and SE-BOLD (dashed line) percent signal changes for the superficial ROI (red) and parenchyma ROI (blue) at 9.4 T (A) and 15.2 T (B), respectively

TABLE 3 ΔR_2^*, ΔR_2, and $\Delta R_2^*/\Delta R_2$ from total, superficial, and parenchyma ROIs

Magnetic field	Echo type	Total S1FL	Superficial ROI[a]	Parenchyma ROI[a]	Super/par ratio[b]
9.4 T	$-\Delta R_2^*$	1.72 ± 0.13	2.38 ± 0.23‡	1.41 ± 0.13	1.76 ± 0.18
	$-\Delta R_2$	1.19 ± 0.09	1.31 ± 0.13	1.13 ± 0.09	1.19 ± 0.11
	$\Delta R_2^*/\Delta R_2$	1.51 ± 0.15	1.95 ± 0.27†	1.32 ± 0.15	1.58 ± 0.23
15.2 T	$-\Delta R_2^*$	3.09 ± 0.35	4.15 ± 0.44‡	2.59 ± 0.34	1.73 ± 0.15
	$-\Delta R_2$	1.97 ± 0.15	2.13 ± 0.22	1.88 ± 0.14	1.13 ± 0.08
	$\Delta R_2^*/\Delta R_2$	1.62 ± 0.18	2.13 ± 0.28‡	1.40 ± 0.17	1.57 ± 0.15
15.2 T/9.4 T	ΔR_2^*	1.80	1.74	1.84	0.95
	ΔR_2	1.66	1.63	1.66	0.98
	$\Delta R_2^*/\Delta R_2$	1.07	1.09	1.06	1.03

Unit of ΔR_2^* and ΔR_2 is sec^{-1}.

[a]Statistical analyses were performed between superficial and parenchyma ΔR_2^*, ΔR_2, and $\Delta R_2^*/\Delta R_2$ with paired t-test (†$P < 0.05$; ‡$P < 0.01$).

[b]No field-dependent statistical significance was found in the superficial-to-parenchyma ratio.

with B_0; (2) BOLD percent signal changes are slightly higher at 15.2 T than at 9.4 T when TE = tissue T_2^* (T_2); and (3) SE-BOLD signals are similar in the both surface and parenchymal regions, whereas GE-BOLD signals are higher at the surface region than at the parenchymal region.

The measured BOLD signal is a sum of the intravascular (IV) and EV signals. The IV contribution is dependent on blood and tissue relaxation times as well as TE. Blood T_2 is dependent on magnetic field strength and oxygenation level, and can be estimated (Equations 6 and 7 of Uldağ et al[14]). Blood T_2 is 4.9 and 7.9 ms at 9.4 T and 2.0 and 3.3 ms at 15.2 T for an oxygenation level of 0.6 and 0.7, respectively, whereas tissue T_2 is 35.7 ms at 9.4 T and 24.5 ms at 15.2 T. Then, the intravascular contribution can be estimated as a function of TE at different magnetic fields (see Figure 1 in Duong et al[12]). In our experimental parameters for both magnetic fields, the IV BOLD signal is minimal and the EV BOLD signal is dominant.

4.1 | Comparison with previous field-dependent studies

Uldağ et al[14] reported comprehensive simulation data for field-dependent GE- and SE-BOLD signals. When TE = tissue T_2^*, the GE-BOLD signal increases with field strength linearly for capillaries and sublinearly for venules, but decreases with field strength linearly for arterioles (see Figure 5A in Uldağ et al[14]); consequently, the GE-BOLD signal slightly increases for total microvasculature with field strength at $B_0 > 9.4$ T. When TE = tissue T_2, the SE-BOLD signal increases with field strength linearly for capillaries, but decreases with field strength for arterioles and venules (see Figure 3B in Uldağ et al[14]); consequently, SE-BOLD is similar for total microvasculature with field strength at $B_0 > 9.4$ T. In order to calculate only EV BOLD signals at TE = T_2^* or T_2, experimentally determined ΔR_2^* and ΔR_2 were multiplied by baseline T_2^* and T_2, respectively. When TE = tissue T_2^* and T_2, the BOLD percent signal change is 4.6% and 5.3% for GE-BOLD and 4.3% and 4.8% for SE-BOLD at 9.4 T and 15.2 T, respectively. Our data generally agree with previously reported comprehensive simulation data in Uldağ et al.[14]

The ΔR_2^* ratio of 15.2 T to 9.4 T was 1.8 in S1FL ROI, which is supralinear to B_0, but ΔR_2 ratio was 1.66, which is linear to B_0. It is often thought that SE-BOLD is diffusion sensitive and quadratic to magnetic field strength, whereas GE-BOLD is linear to quadratic to B_0, based on earlier simulation studies.[5] But this expectation is only valid for low fields of <4 T. Susceptibility-induced ΔR_2 increases with vessel size, peaks at a maximally sensitive tuning diameter, and decreases for larger sizes. Larger susceptibility effects (induced by higher B_0) shift a tuning diameter to a smaller size. Thus, ΔR_2 is supralinear to B_0 for vessels sized smaller than the tuning diameter, but sublinear for vessels sized larger than the tuning diameter. Linear field-dependent ΔR_2 ratio of 15.2 T to 9.4 T can be explained by shifted tuning diameter to capillaries at ultrahigh fields.

Seehafer et al[13] investigated field and echo-type dependency of BOLD fMRI with the same forepaw stimulation rat model. BOLD percent signal changes at the same TE (16 msec for GE and 25 msec for SE) were found to be similar between 7 T and 11.7 T in GE- and SE-BOLD fMRI. The average BOLD signal was 1.5% to 1.8% for both magnetic fields, and GE-/SE-BOLD ratio was close to be ~1.0 in both fields (corresponding to $\Delta R_2^*/\Delta R_2 \approx 1.56$). Given that higher magnetic fields induce higher EV and less IV BOLD signals, the similar BOLD response at the 2 magnetic fields may be explained by a match between an increase in the EV BOLD signal and a decrease in the IV signal at 11.7 T. Assuming that the SE BOLD signal of 1.5% at 11.7 T completely originates from the EV compartment and the EV BOLD response is linearly dependent on B_0, the EV BOLD signal at 7 T is expected to be 0.9%. The IV BOLD signal at 7 T can be estimated from tissue T_2 of 50 msec and blood T_2 change from 8.5 msec (an oxygenation level of 0.6) to 13.4 msec (an oxygenation level of 0.7).[14] At the TE of 25 msec, the IV BOLD signal is 0.5% and 0.9% for CBV of 3% and 5%, respectively. Thus, the total SE BOLD signal at 7 T will be 1.4% to 1.8%, which can explain the experimental 7 T BOLD signal of 1.7% (see Table 2 in Seehafer et al[13]). In our 9.4 T versus 15.2 T studies, our experimental data can be easily explained by the dominant EV BOLD contribution.

4.2 | Poststimulus BOLD undershoots at ultrahigh fields

Poststimulus undershoots were observed in averaged time courses (Figure 2). Poststimulus undershoots were 4 to 6 times smaller than the positive BOLD response. Because of small poststimulus undershoot magnitudes, echo time and field dependency is not obvious (see Supporting Information Table S1), even though it has a linear trend. The exact source of the BOLD poststimulus undershoot is controversial. One or more physiological factors may contribute to a poststimulus BOLD undershoot, including a poststimulus cerebral blood flow undershoot,[31–33] a slow poststimulus return of venous CBV to baseline,[34–37] and/or a slow poststimulus return of cerebral metabolic rate of oxygen–related oxygenation values to baseline.[37–39] Exact contributors of the poststimulus undershoot may also depend on stimulus type and duration.

4.3 | TE- and field-dependence of BOLD CNR

For fMRI studies, statistical values (t-value) have been used for selecting activation voxels and are directly related to stimulation-induced signal change to baseline fluctuation ratio,

which is commonly referred to as CNR. It is expected that the highest CNR occurs when TE = T_2^* or T_2. However, we did not observe TE-dependent CNR within our experimental TE range. It is noted that 9.4 T GE-BOLD with TE = 20 and 25 msec has higher CNR than that with TE of 15 msec, albeit of no statistical significance. The reason not to observe significant difference of CNRs across different TEs can be attributed to non-TE-dependent BOLD contribution and insufficient signal averaging.

As expected, GE-BOLD has higher CNR than SE-BOLD fMRI regardless of magnetic field strength. The GE-BOLD contrast has contributions from all sized venous vessels, whereas SE-BOLD has contributions from mostly microvessels. Thus, the GE-BOLD contrast has always higher CNR than SE-BOLD.

In our 9.4 T versus 15.2 T BOLD studies, we observed similar statistical values, even though direct comparison between 2 magnetic fields is not straightforward because of the usage of different coils. Functional sensitivity (eg, statistical value) is directly related to the percent signal change multiplied by temporal signal-to-noise ratio (tSNR; mean sensitivity/temporal noise). Temporal noise is a sum of thermal and system noise and physiological noise contributions. Signal-to-noise ratio (SNR) increases with magnetic field as B_0 to $B_0^{7/4}$, as previously described.[40] Thus, MRI will have 1.6 to 2.3 times higher SNR at 15.2 T than at 9.4 T. When SNR increases with B_0 and/or voxel volume, tSNR increases linearly with SNR of < 50 and reaches a plateau above SNR of ~ 100.[41] Physiological noises are dominant for fMRI with high SNR, whereas thermal and system noises are dominant for fMRI with low SNR.[41,42] In our voxel resolution with signal averaging ($0.47 \times 0.47 \times 1.0$ mm^3), we did not observe magnetic field–dependent statistical values between 9.4 T and 15.2 T, which is similar to previous 7 T versus 11.7 T findings with $0.4 \times 0.4 \times 2.0$ mm^3 resolution.[13] These experimental observations are not unexpected given that both stimulation-induced BOLD signals and physiological noises similarly change with B_0. If baseline SNR is poor and thermal noises are dominant, then tSNR increases with image SNR and consequently with B_0. This condition will be achieved at ultrahigh resolution, then it is advantageous to use ultrahigh fields for fMRI studies.

4.4 | Spatial specificity of GE-BOLD and SE-BOLD

The vascular structure of the rat somatosensory cortex should be reviewed before discussing spatial specificity. The superficial ROI contains pial vessels as well as microvessels. Diameter of rat pial venous vessels is up to 300 μm under isoflurane and pentobarbital anesthesia[43,44] and up to 200 μm under medetomidine.[44] Parenchymal vessels consist of penetrating arterioles, emerging venules, and capillaries. Diameter of emerging venules in the rat S1FL is up to 50 μm, and mostly ranges between 10 and 20 μm under isoflurane.[45] The mean diameter of capillaries in rats is reported to be 3.2 μm[46] to 5.0-5.1 μm.[47]

GE-BOLD contrast has been used in high-resolution fMRI studies because it is easy to implement and yields a high CNR. However, GE-BOLD contrast contains significant contributions from large draining veins,[48–50] whereas SE-BOLD is much less sensitive to macrovessels than GE-BOLD.[14,18,51] This issue has been examined by comparing BOLD signals of the microvessel-dominant parenchyma ROI and macrovessel-containing superficial ROI. The ΔR_2^* ratio of superficial to parenchyma region was 1.76 and 1.73 at 9.4 T and 15.2 T, respectively, whereas corresponding ΔR_2 ratio was 1.19 and 1.13 at 9.4 T and 15.2 T, respectively (Table 3). This clearly demonstrates that SE-BOLD contrast is less sensitive to large pial vessels than GE-BOLD, as expected. When large vessel regions are active during stimulation, the SE-BOLD technique is more suitable than GE-BOLD for submillimeter high-resolution brain mapping.

EV $\Delta R_2^*/\Delta R_2$ ratio is closely related to a weighted mean vessel size. Our $\Delta R_2^*/\Delta R_2$ at 9.4 T was 1.51 for the total S1FL ROI and 1.32 for the parenchymal ROI. To explain a mean vessel size, it is necessary to measure $\Delta R_2^*/\Delta R_2$ during a change in blood susceptibility effect without blood volume change,[51] which can be achieved with the use of contrast agents such as iron oxides and oxygen. In the cat visual cortex, $\Delta R_2^*/\Delta R_2$ at 9.4 T was 3.3 for the total visual ROI[23,24] and 1.7 to 1.9 for the parenchymal ROI.[23,26] In the human motor cortex, $\Delta R_2^*/\Delta R_2$ at 9.4 T was 3.0 during finger movements.[27] Different species have different vascular density and diameter distributions. A less $\Delta R_2^*/\Delta R_2$ in rats than in cats and humans may be explained by a smaller weighted mean vessel diameter.

5 | CONCLUSION

Our systematic measurements of GE- and SE-BOLD fMRI at 9.4 T and 15.2 T demonstrate that ultrahigh fields increase functional ΔR_2^* and ΔR_2, and that SE-BOLD fMRI improves spatial specificity to microvessels. Percent change of GE-BOLD and SE-BOLD at the optimal echo time is slightly higher at 15.2 T than at 9.4 T. The ultrahigh field of 15.2 T will be advantageous only for thermal-noise–dominant ultrahigh resolution fMRI.

ACKNOWLEDGMENTS

This work was supported by the Institute for Basic Science (IBS-R015-D1). We thank Drs Kamil Uludağ, Seiji Ogawa, and Kazuto Masamoto for helpful discussions and Mr Chanhee Lee for maintenance of MR instruments.

REFERENCES

1. Ogawa S, Lee TM, Kay A, Tank D. Brain magnetic resonance imaging with contrast dependent on blood oxygenation. *Proc Natl Acad Sci U S A*. 1990;87:9868-9872.
2. Bandettini PA, Wong EC, Hinks RS, Tikofsky RS, Hyde JS. Time course EPI of human brain function during task activation. *Magn Reson Med*. 1992;25:390-397.
3. Kwong KK, Belliveau JW, Chesler DA, et al. Dynamic magnetic resonance imaging of human brain activity during primary sensory stimulation. *Proc Natl Acad Sci U S A*. 1992;89:5675-5679.
4. Ogawa S, Tank DW, Menon R, et al. Intrinsic signal changes accompanying sensory stimulation: functional brain mapping with magnetic resonance imaging. *Proc Natl Acad Sci U S A*. 1992;89:5951-5955.
5. Ogawa S, Menon RS, Tank DW, et al. Functional brain mapping by blood oxygenation level-dependent contrast magnetic resonance imaging. *Biophys J*. 1993;64:803-812.
6. Boxerman JL, Hamberg LM, Rosen BR, Weisskoff RM. MR contrast due to intravascular magnetic susceptibility perturbations. *Magn Reson Med*. 1995;34:555-566.
7. Ogawa S, Menon RS, Kim SG, Ugurbil K. On the characteristics of functional magnetic resonance imaging of the brain. *Annu Rev Biophys Biomol Struct*. 1998;27:447-474.
8. Kim SG, Ogawa S. Biophysical and physiological origins of blood oxygenation level-dependent fMRI signals. *J Cereb Blood Flow Metab*. 2012;32:1188-1206.
9. Turner R, Jezzard P, Wen H, et al. Functional mapping of the human visual cortex at 4 Tesla and 1.5 Tesla using deoxygenation contrast EPI. *Magn Reson Med*. 1993;29:277-279.
10. Yang Y, Wen H, Mattay VS et al. Comparison of 3D BOLD functional MRI with spiral acquisition at 1.5 and 4.0 T. *Neuroimage*. 1999;9:446-451.
11. Gati JS, Menon RS, Uğurbil K, Rutt BK. Experimental determination of the BOLD field strength dependence in vessels and tissue. *Magn Reson Med*. 1997;38:296-302.
12. Duong TQ, Yacoub E, Adriany G, Hu X, Uğurbil K, Kim SG. Microvascular BOLD contribution at 4 and 7 T in the human brain: gradient-echo and spin-echo fMRI with suppression of blood effects. *Magn Reson Med*. 2003;49:1019-1027.
13. Seehafer JU, Kalthoff D, Farr TD, Wiedermann D, Hoehn M. No increase of the blood oxygenation level-dependent functional magnetic resonance imaging signal with higher field strength: implications for brain activation studies. *J Neurosci*. 2010;30:5234-5241.
14. Uludağ K, Müller-Bierl B, Uğurbil K. An integrative model for neuronal activity-induced signal changes for gradient and spin echo functional imaging. *Neuroimage*. 2009;48:150-165.
15. Weisskoff R, Zuo CS, Boxerman JL, Rosen BR. Microscopic susceptibility variation and transverse relaxation: theory and experiment. *Magn Reson Med*. 1994;31:601-610.
16. Bandettini PA, Wong EC. Effects of biophysical and physiologic parameters on brain activation-induced R2* and R2 changes: simulations using a deterministic diffusion model. *Int J Imaging Syst Technol*. 1995;6:133-152.
17. Kennan RP, Zhong J, Gore JC. Intravascular susceptibility contrast mechanisms in tissues. *Magn Reson Med*. 1994;31:9-21.
18. Lee SP, Silva AC, Ugurbil K, Kim SG. Diffusion-weighted spin-echo fMRI at 9.4 T: microvascular/tissue contribution to BOLD signal changes. *Magn Reson Med*. 1999;42:919-928.
19. Ueki M, Miles G, Hossmann KA. Effect of alpha-chloralose, halothane, pentobarbital and nitrous oxide anesthesia on metabolic coupling in somatosensory cortex of rat. *Acta Anaesthesiol Scand*. 1992;36:318-322.
20. Gyngell ML, Bock C, Schmitz B, Hoehn-Berlage M, Hossmann KA. Variation of functional MRI signal in response to frequency of somatosensory stimulation in α-chloralose anesthetized rats. *Magn Reson Med*. 1996;36:13-15.
21. Hyder F, Behar KL, Martin MA, Blamire AM, Shulman RG. Dynamic magnetic resonance imaging of the rat brain during forepaw stimulation. *J Cereb Blood Flow Metab*. 1994;14:649-655.
22. Silva AC, Lee SP, Yang G, Iadecola C, Kim SG. Simultaneous blood oxygenation level-dependent and cerebral blood flow functional magnetic resonance imaging during forepaw stimulation in the rat. *J Cereb Blood Flow Metab*. 1999;19:871-879.
23. Zhao F, Wang P, Kim SG. Cortical depth-dependent gradient-echo and spin-echo BOLD fMRI at 9.4T. *Magn Reson Med*. 2004;51:518-524.
24. Zhao F, Wang P, Hendrich K, Ugurbil K, Kim SG. Cortical layer-dependent BOLD and CBV responses measured by spin-echo and gradient-echo fMRI: insights into hemodynamic regulation. *Neuroimage*. 2006;30:1149-1160.
25. Bandettini PA, Wong EC, Jesmanowicz A, Hinks RS, Hyde JS. Spin-echo and gradient-echo epi of human brain activation using bold contrast: a comparative study at 1.5 T. *NMR Biomed*. 1994;7:12-20.
26. Jin T, Wang P, Tasker M, Zhao F, Kim SG. Source of nonlinearity in echo-time-dependent BOLD fMRI. *Magn Reson Med*. 2006;55:1281-1290.
27. Budde J, Shajan G, Zaitsev M, Scheffler K, Pohmann R. Functional MRI in human subjects with gradient-echo and spin-echo EPI at 9.4 T. *Magn Reson Med*. 2014;71:209-218.
28. Jones RA, Schirmer T, Lipinski B, Elbel GK, Auer DP. Signal undershoots following visual stimulation: a comparison of gradient and spin-echo BOLD sequences. *Magn Reson Med*. 1998;40:112-118.
29. Bandettini PA, Jesmanowicz A, Wong EC, Hyde JS. Processing strategies for time course data sets in functional MRI of the human brain. *Magn Reson Med*. 1993;30:161-173.
30. Paxinos G, Watson C. *The Rat Brain in Stereotaxic Coordinates*. 6th ed. New York, NY: Academic; 2005.
31. Hoge RD, Atkinson J, Gill B, Crelier GR, Marrett S, Pike GB. Stimulus-dependent BOLD and perfusion dynamics in human V1. *Neuroimage*. 1999;9:573-585.
32. Jin T, Kim SG. Cortical layer-dependent dynamic blood oxygenation, cerebral blood flow and cerebral blood volume responses during visual stimulation. *Neuroimage*. 2008;43:1-9.
33. Chen JJ, Pike GB. Origins of the BOLD post-stimulus undershoot. *Neuroimage*. 2009;46:559-568.
34. Kim T, Kim SG. Temporal dynamics and spatial specificity of arterial and venous blood volume changes during visual stimulation: implication for bold quantification. *J Cereb Blood Flow Metab*. 2011;31:1211-1222.
35. Mandeville JB, Marota JJ, Kosofsky BE, et al. Dynamic functional imaging of relative cerebral blood volume during rat forepaw stimulation. *Magn Reson Med*. 1998;39:615-624.
36. Chen JJ, Pike GB. BOLD-specific cerebral blood volume and blood flow changes during neuronal activation in humans. *NMR Biomed*. 2009;22:1054-1062.

37. Hua J, Qin Q, Pekar JJ, van Zijl PC. Measurement of absolute arterial cerebral blood volume in human brain without using a contrast agent. *NMR Biomed*. 2011;24:1313-1325.
38. Frahm J, Krüger G, Merboldt KD, Kleinschmidt A. Dynamic uncoupling and recoupling of perfusion and oxidative metabolism during focal brain activation in man. *Magn Reson Med*. 1996;35:143-148.
39. Zhao F, Jin T, Wang P. Kim SG, Improved spatial localization of post-stimulus BOLD undershoot relative to positive BOLD. *Neuroimage*. 2007;34:1084-1092.
40. Moser E, Laistler E, Schmitt F, Kontaxis G. Corrigendum: ultra-high field NMR and MRI—the role of magnet technology to increase sensitivity and specificity. *Front Phys*. 2017;5:41.
41. Triantafyllou C, Hoge RD, Krueger G, et al. Comparison of physiological noise at 1.5 T, 3 T and 7 T and optimization of fMRI acquisition parameters. *Neuroimage*. 2005;26:243-250.
42. Bodurka J, Ye F, Petridou N, Murphy K, Bandettini PA. Mapping the MRI voxel volume in which thermal noise matches physiological noise-Implications for fMRI. *Neuroimage*. 2007;34:542-549.
43. Vovenko E. Distribution of oxygen tension on the surface of arterioles, capillaries and venules of brain cortex and in tissue in normoxia: an experimental study on rats. *Pflugers Arch Eur J Physiol*. 1999;437:617-623.
44. Fukuda M, Vazquez AL, Zong X, Kim SG. Effects of the α2-adrenergic receptor agonist dexmedetomidine on neural, vascular and BOLD fMRI responses in the somatosensory cortex. *Eur J Neurosci*. 2013;37:80-95.
45. Park SH, Masamoto K, Hendrich K, Kanno I, Kim SG. Imaging brain vasculature with BOLD microscopy: MR detection limits determined by in vivo two-photon microscopy. *Magn Reson Med*. 2008;59:855-865.
46. Hutchinson EB, Stefanovic B, Koretsky AP, Silva AC. Spatial flow-volume dissociation of the cerebral microcirculatory response to mild hypercapnia. *Neuroimage*. 2006;32:520-530.
47. Bär T. The vascular system of the cerebral cortex. *Adv Anat Cell Biol*. 1980;59:1-62.
48. Frahm J, Merboldt KD, Hänicke W, Kleinschmidt A, Boecker H. Brain or vein—oxygenation or flow? On signal physiology in functional MRI of human brain activation. *NMR Biomed*. 1994;7:45-53.
49. Kim SG, Hendrich K, Hu X, Merkle H, Ugurbil K. Potential pitfalls of functional MRI using conventional gradient-recalled echo techniques. *NMR Biomed*. 1994;7:69-74.
50. Turner R. How much cordex can a vein drain? Downstream dilution of activation-related cerebral blood oxygenation changes. *Neuroimage*. 2002;16:1062-1067.
51. Dennie J, Mandeville JB, Boxerman JL, Packard SD, Rosen BR, Weisskoff RM. NMR imaging of changes in vascular morphology due to tumor angiogenesis. *Magn Reson Med*. 1998;40:793-799.

SUPPORTING INFORMATION

Additional Supporting Information may be found online in the supporting information tab for this article.

FIGURE S1 (A) A design of a home-built rat cradle with Autodesk Fusion 360. (B) A picture of a home-built rat cradle containing 2 ear bars, 1 bite bar, and a mask for fixation of rat head. (C) Demonstration of the use of a rat cradle using a rat. A surface coil was used to maximize a sensitivity to a specific region of brain.

FIGURE S2 Statistical activation maps from 3 TEs GE- and SE-BOLD overlaid on the corresponding BOLD images at 9.4 T (A) and 15.2 T (B). Color bar represents the cross-correlation values.

TABLE S1 Poststimulus undershoot GE- and SE-BOLD percent signal changes at 9.4 T and 15.2 T.

How to cite this article: Han S, Son JP, Cho H, Park J-Y, Kim S-G. Gradient-echo and spin-echo blood oxygenation level–dependent functional MRI at ultrahigh fields of 9.4 and 15.2 Tesla. *Magn Reson Med*. 2019;81:1237–1246. https://doi.org/10.1002/mrm.27457